https://doi.org/10.5194/acp-2019-815
Preprint. Discussion started: 23 October 2019

Atmospheric Chemistry and Physics
Open Access
Discussions

Improved 1-km-resolution $PM_{2.5}$ estimates across China using the space-time extremely randomized trees

Jing Wei[1], Zhanqing Li[2*], Wei Huang[3], Wenhao Xue[1], Lin Sun[4], Jianping Guo[5], Yiran Peng[6], Jing Li[7], Alexei Lyapustin[8], Lei Liu[9], Hao Wu[1], Yimeng Song[10]

1. State Key Laboratory of Remote Sensing Science, College of Global Change and Earth System Science, Beijing Normal University, Beijing, China
2. Department of Atmospheric and Oceanic Science, Earth System Science Interdisciplinary Center, University of Maryland, College Park, MD, USA
3. State Key Laboratory of Remote Sensing Science, Faculty of Geographical Science, Beijing Normal University, Beijing, China
4. College of Geomatics, Shandong University of Science and Technology, Qingdao, China
5. State Key Laboratory of Severe Weather, Chinese Academy of Meteorological Sciences, Beijing, China
6. Ministry of Education Key Laboratory for Earth System Modeling, Department of Earth System Science, Tsinghua University, Beijing, China
7. Department of Atmospheric and Oceanic Sciences, School of Physics, Peking University, Beijing, China
8. Laboratory for Atmospheres, NASA Goddard Space Flight Center, Greenbelt, Maryland, USA
9. College of Earth and Environmental Sciences, Lanzhou University, Lanzhou, China
10. Department of Urban Planning and Design, Faculty of Architecture, The University of Hong Kong, Hong Kong

Correspondence to: Zhanqing Li (zli@atmos.umd.edu)

Abstract

Fine particulate matter with aerodynamic diameters ≤ 2.5 μm ($PM_{2.5}$) shows adverse effects on human health and atmospheric environment. Satellite-derived aerosol products have been intensively adopted in estimating surface $PM_{2.5}$ concentrations, but most previous studies failed to monitor air pollution over small-scale areas limited by coarse spatial-resolution (3–50 km) and low data-quality aerosol optical depth (AOD) products. Therefore, a new space-time extremely randomized trees (STET) model is

https://doi.org/10.5194/acp-2019-815
Preprint. Discussion started: 23 October 2019

developed that integrates spatiotemporal information to improve $PM_{2.5}$ estimates at both spatial resolution and overall accuracy across China. To this end, the newly released MODIS MAIAC AOD product, meteorological and other auxiliary data are inputs to the STET model. Daily 1-km $PM_{2.5}$ maps in 2018 across mainland China are produced. The STET model performs well with a high out-of-sample (out-of-station) cross-validation coefficient of 0.89 (0.88), a low root-mean-square error of 10.35 (10.97) μg/m^3, a small mean absolute error of 6.71 (7.17) μg/m^3, and a small mean relative error of 21.37 % (23.77%), respectively. Particularly, it can well capture the $PM_{2.5}$ concentrations at both regional and individual site scales. In addition, it posed a strong predictive power (e.g., monthly-R^2 = 0.80) and can be used to predict the historical $PM_{2.5}$ records. The North China Plain, the Sichuan Basin, and Xinjiang Province always are featured with high $PM_{2.5}$ pollution, especially in winter. The STET model outperforms most models presented in previous related studies. More importantly, our study provides a new approach to obtain high-quality $PM_{2.5}$ estimates, which is important for air pollution studies over urban areas.

1. Introduction

Atmospheric particulate matter is a relatively stable suspension system with solid and liquid particulate matter evenly dispersed. Fine particles are those particles in ambient air with aerodynamic diameters no more than 2.5 micrometers ($PM_{2.5}$). Compared to coarser particles, $PM_{2.5}$ are rich in toxic and harmful substances and can directly enter the respiratory tract and alveoli of humans. Moreover, they have a long residence time and long transmission distance in the atmosphere (Aggarwal and Jain, 2015). Numerous studies have illustrated that high $PM_{2.5}$ concentration adversely affects human health (Peng et al., 2009; Bartell et al., 2013; Chowdhury and Dey, 2016; Crippa et al., 2019; Song et al., 2019), severely impairs the atmospheric environment (Li et al., 2017), and even significantly influences the cloud and precipitation systems by aerosol radiative and microphysical effects (Koren et al., 2014; Li et al., 2016; Seinfeld et al., 2016; Ceca et al., 2018). Silva et al. (2013) have shown that about 2.1 million people have died each year, resulting from the increasing $PM_{2.5}$ around the world.

Nowadays, air pollution is becoming more severe due to continuously increasing anthropogenic aerosols in developing countries, especially in China (He et al., 2011; Huang et al., 2014; Liu et al., 2017; Zhai et al., 2019). Fine particulate matters have become the primary pollutant in urban environment, garnering much scrutiny from the public (Han et al., 2014; Sun et al., 2016; Wu et al., 2018). Therefore, China Meteorological Administration began to establish ground $PM_{2.5}$ observation network to monitor the urban air quality as early as 2004 (Guo et al., 2009), followed by a denser network established by the Chinese Ministry of Environmental Protection since 2013. However, station-based monitoring is largely limited by the instruments and climatic conditions and cannot completely reflect air pollution over large areas. Satellite remote sensing technology has led to a variety of operational aerosol products using mature aerosol retrieval algorithms (Levy et al., 2013; Lyapustin et al., 2018), which allows the $PM_{2.5}$ estimations at large scale due to their unanimously positive relationships (Guo et al., 2017).

Over the years, numerous approaches have been proposed to improve the $PM_{2.5}$-AOD relationship. Physical models typically construct physical relationships between surface particulate matter concentrations and satellite AOD products through altitude and humidity corrections (Zhang and Li, 2015). Statistical regression models, e.g., the multiple linear regression model, the linear mixed-effect model, the two-stage model, the geographically weighted regression (GWR) model, have been widely used for applications due to their simplicity and versatility (Gupta & Christopher, 2009; Ma et al., 2014; Xiao et al., 2017; Yao et al., 2019). Artificial intelligence models mainly involve the machine learning and deep learning models, e.g., the random forest (RF; Brokamp et al., 2018; Chen et al., 2018; Hu et al., 2017), the extreme gradient boosting model (XGBoost, Chen et al., 2019), the back-propagation and generalized regression neural networks (BRNN and GRNN, Li et al., 2017a).

However, $PM_{2.5}$ is jointly affected by numerous factors, e.g., meteorological conditions, human activities, and topography, showing great spatial and temporal heterogeneities. This makes it difficult for above traditional physical and statistical regression approaches to accurately explain and construct $PM_{2.5}$-AOD relationships, leading to poor $PM_{2.5}$ estimates. Despite stronger data mining ability, most artificial intelligence approaches have been simplistically adopted in $PM_{2.5}$ predictions, neglecting their crucial spatiotemporal characteristics (Chen et al., 2018, 2019; Hu et al., 2017; Li et al., 2017a; Brokamp et al., 2018; Xue et al., 2019). Furthermore, deep learning is highly dependent on the computer performance and is less computationally efficient. On the other hand, most widely used

https://doi.org/10.5194/acp-2019-815
Preprint. Discussion started: 23 October 2019

aerosol products are generated with low spatial resolutions (3–50 km), and thus are seriously limited for applications over small-scale regions such as urban areas.

Focus on these problems, to address the spatiotemporal heterogeneity and improve $PM_{2.5}$ estimates, a new space-time extremely randomized trees (STET) model is developed using the MODIS MAIAC AOD product at 1-km resolution associated with meteorological, land-use, topographic, and population parameters. Then the space continuous 1-km $PM_{2.5}$ maps at different temporal scales covering mainland China in 2018 are generated. Section 2 describes the data sources and integration. Section 3 introduces the space-time extremely randomized trees (STET) model, and section 4 presents the validation and comparison of our $PM_{2.5}$ estimates across China. Section 5 gives a summary and conclusion.

2. Data sources

2.1 $PM_{2.5}$ ground measurements

In this study, the hourly in-situ $PM_{2.5}$ observations at 1583 monitoring stations (Figure 1) across mainland China from 1, January 2017 to 31, December 2018 are collected, and they are then averaged to obtain the daily $PM_{2.5}$ measurements. The $PM_{2.5}$ observations are measured using the tapered element oscillating microbalance approach method or β-attenuation monitors that have undergone further calibration and strict quality control procedures (Guo et al., 2009).

[Please insert Figure 1 here]

2.2 MAIAC AOD product

The MAIAC algorithm was developed and applied to generate MODIS aerosol products from darkest to brightest surfaces at a 1-km spatial resolution over land (Lyapustin et al., 2011). On 30 May 2018, official 1-km-resolution MAIAC aerosol products were released and made freely available to all users. This dataset is produced using the revised MAIAC algorithm with continuous improvements in scale transition using spectral regression coefficients, cloud detection, determination of aerosol models, over-water processing, and general optimization in the global aerosol retrieval process (Lyapustin et al., 2018). MAIAC daily aerosol products from Terra and Aqua satellites are collected in 2018 across

https://doi.org/10.5194/acp-2019-815
Preprint. Discussion started: 23 October 2019

Atmospheric Chemistry and Physics Discussions
Open Access

China, and the 550-nm AOD retrievals with high quality assurance ($QA_{CloudMask}$ = Clear and $QA_{AdjacencyMask}$ = Clear) are used.

2.3 Auxiliary data

The auxiliary data mainly includes meteorological, land-cover, surface topographic, and population data. The meteorological variables are collected from ERA-Interim atmospheric reanalysis products, including the boundary layer height (BLH), evaporation (EP), temperature (TEM), precipitation (PRE), relative humidity (RH), surface pressure (SP), wind speed (WS), and wind direction (WD). For meteorological variables, the observations between 1000 to 1400 local time are averaged to be consistent with satellite overpass times. The land-cover data include the MODIS land use cover and NDVI products. The topographic data include the surface elevation, slope, aspect, and relief (Wei et al., 2019a), are calculated from the SRTM DEM product, and the population derived from VIIRS nighttime lights data. Table 1 provides detailed information about the data sources.

[Please insert Table 1 here]

2.4 Data integration

Terra and Aqua MAIAC AOD products have different spatial coverages due to frequent clouds and difference in their respective imaging times. Therefore, both Terra and Aqua MAIAC datasets are combined and merged through the linear regression approach (Eq. 1) to reduce the systematic differences and enlarge the spatial coverage. By integrating the two datasets, the spatial coverage is greatly increased by more than 15% over most areas across China, which can lead to wider spatial-coverage $PM_{2.5}$ maps. More importantly, the number of valid data samples has significantly increased by approximately 25–32% after combination than just using Terra or Aqua MAIAC products, which can improve the model training ability.

$$\begin{cases} \tau_T = k_1 \cdot \tau_A + b_1 \\ \tau_A = k_2 \cdot \tau_T + b_2 \\ \tau_C = \mathrm{mean}(\tau_T, \tau_A) \end{cases} \quad (1)$$

where τ_T, τ_A, and τ_C denote the Terra, Aqua, and combined AODs.

https://doi.org/10.5194/acp-2019-815
Preprint. Discussion started: 23 October 2019

In addition, due to different spatial resolutions, all the 16 auxiliary variables are uniformly aggregated to a 1-km (≈ 0.01° × 0.01°) spatial resolution using the bilinear interpolation approach. After removing invalid or unrealistic values, there are 167,716 matched $PM_{2.5}$-AOD samples and independent variables are collected for 2018 in China.

3. Space-time extremely randomized trees

In this study, a tree-based ensemble learning approach, called the extremely randomized trees (ET), is selected to deal with complex supervised regression issues and to construct robust $PM_{2.5}$-AOD relationships. Compared to other tree-based ensemble approaches (e.g., RF), this model splits nodes by completely randomly selecting cut-points and uses all the training sample learning sample (instead of the bootstrap approach) to grow trees. Therefore, it is with stronger randomness and can efficiently solves variance problems and mines valuable information (Geurts et al., 2006). There are four key steps during the splitting process with the training dataset *S*:

(a) Split a node (*S*). *K* attributes (a_1, …, a_K) are selected from all independent attributes in the local training subset *S*; and then *K* splits (s_1, …, s_k) are drawn;

(b) Pick a random split. A subset *S* and an attribute *a* are used as inputs to calculate the maximum (a_{max}) and minimum (a_{min}) value; then a random cut-point a_c uniformly in (a_{max}, a_{min}) is drawn; and if $a < a_c$, the split s_i (i = [1, k]) is returned;

(c) Calculate the score. The score for a split s_i in a subset *S* is measured by Equation 2. If the split s_i satisfy that Score(s^*, *S*) = max{Score(s_i, *S*)}, the split s^* is returned.

(d) Stop the spilt. If |*S*| < n_{min}, or all attributes or the output are constant in in subset *S*, then output a Boolean (i.e., TRUE).

$$Score(s_i, S) = \frac{var\{y|S\} - \frac{|S_l|}{S} var\{y|S_l\} - \frac{|S_r|}{S} var\{y|S_r\}}{var\{y|S\}} \quad (2)$$

where S_l and S_r represents two subsets related to the two outcomes of a split (*s*), and var{} represents the variance of the output *y* in the training set *S*.

https://doi.org/10.5194/acp-2019-815
Preprint. Discussion started: 23 October 2019

Atmospheric Chemistry and Physics
Open Access
Discussions

In the splitting process of the ET model for numerical attributes, K and n_{min} are the two main parameters, which represents the number of attributes randomly selected at each node and the minimum sample size for splitting a node (Geurts et al., 2006), respectively. They are used to establish an ensemble model with the full training samples by building numerous extra-trees. Last, the estimations of these extra-trees are summarized through the arithmetic average in regression problems to obtain the result.

3.1 Model development

Specifically, spatiotemporal heterogeneities, i.e., strong spatial autocorrelation and obvious temporal differences, is the key characteristic of $PM_{2.5}$, presenting great challenges and usually neglected in most regression and artificial intelligence models. Therefore, in this study, a new space-time extremely randomized trees (STET) model, which introduces both the spatial and temporal information, is developed to solve this problem. The spatial (Space) information is represented by the geographical difference between two pixels calculated using the Haversine approach based on their longitude and latitude information (Eq.3), and the temporal (Time) information is represented by the time difference for a given pixel on different days in a year (Eq.5). These two space-time terms can better distinguish and represent the spatiotemporal autocorrelations of $PM_{2.5}$ between different pixels on different polluted days.

$$P_{S(i,j,t)} = f(Lon_{i,j,t}, Lat_{i,j,t}) = haversin(\triangle\alpha) + \cos(\alpha_1)\cos(\alpha_2)\, haversin(\triangle\beta) \quad (3)$$

$$haversin(\theta) = sin^2(\theta/2) = [1 - \cos(\theta)]/2 \quad (4)$$

$$P_{T(i,j,t)} = DOY_{i,j,t} \quad (5)$$

where $P_{x(i,j,t)}$ represents a given pixel at location (i, j) in the year t, and DOY represents the day of year; α_1 and α_2 denote the latitude of two points, and $\triangle\alpha$ and $\triangle\beta$ denote the latitude and longitude difference between two points in space. Therefore, surface measured $PM_{2.5}$ concentrations, MAIAC AODs, meteorological conditions, land cover, topographic conditions, population, and spatiotemporal information are used as preliminary inputs for the STET model.

3.2 Model adjustment

https://doi.org/10.5194/acp-2019-815
Preprint. Discussion started: 23 October 2019

However, due to a large number of independent variables considered, this will lead to the unavoidable over-fitting issue during the model training process. Therefore, the model need be further adjusted by selecting more important variables rather than all variables to overcome this issue and improve the model efficiency. For this purpose, the importance scores of all selected independent variables and spatiotemporal information to $PM_{2.5}$ estimates for the STET model are calculated in China (Figure 2). The results suggest that AOD is the most influential variable, contributing ~31% toward daily $PM_{2.5}$ estimates. Time and space terms are the other two important factors, contributing about 9–10%. This further illustrates the importance of spatial and temporal information on $PM_{2.5}$ estimates. Because there is little precipitation on most days throughout the year, PRE contributes little to PM estimates, by contrast, most other meteorological variables contribute more to $PM_{2.5}$ estimates, especially BLH, EP, and TEM with average importance scores of 9%, 8%, and 7%, respectively. The contributions of surface conditions (i.e., LUC, relief, aspect, and slope) and NTL to $PM_{2.5}$ estimates are generally less than 2%. Therefore, these six less important variables are excluded from the STET model and the remaining variables are used to construct the finial $PM_{2.5}$ estimated model.

[Please insert Figure 2 here]

3.3 Model validation

In this study, the widely used 10-fold cross-validation (10-CV) procedure (Rodriguez et al., 2010) is selected for model validation, where all data samples are divided into ten subsets randomly, and nine of them are used as the training data and the remaining is the testing data, indicating that the training and testing data are totally independent. This approach is repeated in turn for ten times. Then the error rate of each test is calculated, and the mean error rate from ten tests determines the final result. Here, the out-of-sample and out-of-station 10-CV procedures are involved, which the former one is performed based on the observations and used to evaluate the overall accuracy of the STET model. However, the later one is performed based on the monitoring stations and used to evaluate the model spatial performance. This means that training and testing are made of different spatial points, and the

https://doi.org/10.5194/acp-2019-815
Preprint. Discussion started: 23 October 2019

relationship between spatial predictors and $PM_{2.5}$ concentrations estimated in the training dataset is then predicted on the testing.

4. Results and discussion

4.1 Validation of MAIAC product

MAIAC AOD retrievals are first evaluated with surface observations using the spatiotemporal matching approach (Wei et al., 2019b) at 18 AERONET monitoring stations in China (Figure 3). The MAIAC AOD retrievals show great performance with small estimation errors across mainland China (Figure 2a) and more than 84% of the matchups satisfy the MODIS expected errors (Levy et al., 2013) at the national scale. Besides vegetated surfaces, e.g., cropland and grassland, the MAIAC algorithm shows a considerable accuracy over heterogeneous urban surfaces (Figure 2b). MAIAC AOD products are more accurate and less biased than the widely used Dark Target (DT) and Deep Blue products at coarse spatial resolutions (N. Liu et al., 2019; Wei et al., 2018; Tao et al., 2019; Zhang et al., 2019). More importantly, the DT algorithm cannot be applied with a large amount of missing values over bright surfaces, and aerosol loadings are significantly overestimated over heterogeneous urban surfaces (Levy et al., 2013; Wei et al., 2018; 2019c). Therefore, the higher data-quality and spatial-resolution MAIAC products, which can generate more accurate and detailed $PM_{2.5}$ estimates, are selected in this study.

[Please insert Figure 3 here]

4.2 Model performance

4.2.1 Spatial-scale validation

Figure 4 shows the sample-based and station-based 10-CV results of daily $PM_{2.5}$ estimates for the traditional ET model and our new developed STET model at the national scale in 2018. The results suggest that the original ET model works well in estimating $PM_{2.5}$ concentrations with an average out-of-sample CV-R^2, of 0.84 and overall small estimation uncertainties. However, when consider the spatiotemporal information, the model performance has been significantly improved with an increasing sample-based CV-R^2 equal to 0.89, a stronger regression line (e.g., slope = 0.86), and decreasing RMSE

https://doi.org/10.5194/acp-2019-815
Preprint. Discussion started: 23 October 2019

(~12.46 μg/m^3), MAE (~8.26 μg/m^3), and MRE (~28.09%) values. Nevertheless, the $PM_{2.5}$ concentrations tend to be overall underestimated at high polluted days ($PM_{2.5}$ > 100 μg/m^3) by the STET model. For the spatial performance, compared to the original ET model, the STET model shows a stronger spatial predictive power with a higher out-of-station CV-R^2 of 0.88, a lower RMSE of 10.97 μg/m^3, MAE of 7.17 μg/m^3, and MRE of 23.77%. These results illustrate that spatiotemporal information are crucial in improving the $PM_{2.5}$-AOD relationships and should be carefully considered when introducing statistical regression models using remote sensing techniques.

[Please insert Figure 4 here]

Figure 5 shows the sample-based 10-CV results of the STET model in $PM_{2.5}$ daily estimates over eastern and western China (according to the widely used Heihe-Tengchong line), and four typical local regions (Figure 1). The STET model performs differently over eastern and western China mainly due to significant differences in land cover and climate conditions. There are 1289 uniformly distributed $PM_{2.5}$ stations in eastern China, and 127,241 daily samples were collected. The STET model performs well eastern China with a high sample-based CV-R^2 equal to 0.90 and low estimation uncertainties, i.e., RMSE = 9.77 μg/m^3, MAE = 6.44 μg/m^3, and MRE = 19.24%. By contrast, there are 294 unevenly and sparsely distributed $PM_{2.5}$ stations in western China, thus about three times fewer daily $PM_{2.5}$ estimates were collected. The model performance is overall poorer (e.g., CV-R^2 = 0.86, and RMSE = 11.99 μg/m^3) than over eastern China. This mainly contributed to brighter surfaces (e.g., desert and bare land) with little vegetation coverage and harsh meteorological conditions over western China.

There were 33,733, 15,199, 6,209, and 6,470 daily samples collected from 233, 184, 95, and 107 uniformly distributed $PM_{2.5}$ monitoring stations in North China Plain (NCP), Yangtze River Delta (YRD), Pearl River Delta (PRD) and Sichuan Basin (SCB), respectively. For former three typical urban agglomerations where people closely concerned, the estimated $PM_{2.5}$ concentrations are highly consistent with surface measurements (CV-R^2 = 0.89–0.92) with overall low estimation uncertainties (i.e., RMSE = 7–12 μg/m^3, MAE = 5–8 μg/m^3, and MRE = 15–19%). In addition, the STET model also performs well over Sichuan Basin with an average CV-R^2 value equal to 0.87 and comparable

https://doi.org/10.5194/acp-2019-815
Preprint. Discussion started: 23 October 2019

estimation uncertainties to North China Plain. In general, despite some differences in model performance, the STET model shows an overall good ability in $PM_{2.5}$ estimates at the regional scale.

[Please insert Figure 5 here]

The national- and regional-scale aggregated evaluations mainly illustrate the overall performance of the STET model in $PM_{2.5}$ estimates, however, due to the inhomogeneity of $PM_{2.5}$ monitoring stations, an additional validation for each monitoring station in China is performed (Figure 6). For statistical significance, only these monitoring stations with more than ten data samples are plotted. The daily $PM_{2.5}$ estimations are well related to surface measurements at most individual stations across China. The average sample-based CV-R^2 is 0.84, and the CV-R^2 values are higher than 0.8 at more than 73% of the monitoring stations, especially for eastern China. However, relatively poorer performances (CV-$R^2 < 0.6$) are observed at some scattered sites located in southwestern and southeastern China. In general, the STET model shows overall low estimation uncertainties at most sites with average RMSE and MAE values of 9.3 and 6.5 μg/m^3, especially for southern China. Moreover, the average RMSE and MAE values are < 10 μg/m^3 at more than 68% and 93% of the monitoring stations across China. Note that these stations show larger RMSE values (> 10 μg/m^3) in central China mainly due to high polluted levels. In addition, the average MRE value is 20.88%, and most stations (> 86%) have low MRE values < 30% in $PM_{2.5}$ estimations in China, especially for those located in eastern and southern China.

[Please insert Figure 6 here]

4.2.2 Temporal-scale validation

Figure 7 shows the STET model performance from all available monitoring stations in China as a function of the day of year. The number of data samples in one day ranges from 54 to 1155 with an average of 466 in 2018. In general, the STET model shows great performance (average CV-R^2 = 0.76) at most days in the year, and more than 76% of the days have CV-R^2 values greater than 0.7. Two main uncertainty metrics, i.e., RMSE and MAE, show similar temporal variations during the year, first decreasing until around day 250 then gradually increasing. In general, approximately equal 92% of the

https://doi.org/10.5194/acp-2019-815
Preprint. Discussion started: 23 October 2019

Atmospheric Chemistry and Physics Discussions

days have low RMSE and MAE values less than 15 and 10 μg/m^3 over the year. Large estimation uncertainties always occur at the beginning and end of the year mainly due to intense human activities and harsh natural environment. Furthermore, MRE is relatively stable ranging from 13% to 52% with an average value of 23.29%, and more than 87% of the days yield low MRE values less than 30% in China. These results illustrate that the STET model show great performance in capturing $PM_{2.5}$ concentrations on most days of the year.

[Please insert Figure 7 here]

Figure 8 shows sample-based cross-validation results for $PM_{2.5}$ daily estimates divided by four seasons in 2018 across China. The results suggest that there are obvious differences in model performance at the seasonal level. The STET model performs best in autumn with the highest CV-R^2 value of 0.90 and strongest regression line (i.e., slope = 0.88, and intercept = 4.88 μg/m^3). The average RMSE, MAE and MRE values are 9.01 μg/m^3, 5.87 μg/m^3, and 21.10 %, respectively. By contrast, the STET model performs worst in summer with the lowest CV-R^2 of 0.76 and smallest slope of 0.74, indicating obvious underestimations. However, summer shows the least amount of air pollution with most daily $PM_{2.5}$ values < 80 μg/m^3, leading to smallest estimation uncertainties. The main reason is that the meteorological conditions in place in summer accelerated the diffusion of pollutants but complicated the $PM_{2.5}$-AOD relationships. The air quality is about two or three times worse in spring and winter than in winter with wider $PM_{2.5}$ ranges and larger standard deviations. Moreover, the STET model shows similar performances in these two seasonal with almost equal CV-R^2 and slope values, as well as close estimation uncertainties.

[Please insert Figure 8 here]

4.2.3 Predictive power

To test the predictive power of the STET model, the model built for the year of 2018 is used to predict the daily $PM_{2.5}$ concentrations in 2017, then validated against the ground measurements from 2017. This approach can ensure the data samples for model training and validation are completely

https://doi.org/10.5194/acp-2019-815
Preprint. Discussion started: 23 October 2019

independent in both spatial and temporal scales. Figure 9 shows the validation of $PM_{2.5}$ predictions in 2017 at different temporal scales across China. The results show that the STET model can correctly capture more than 60% of the historical daily $PM_{2.5}$ concentrations (N = 17,7616). The monthly (N = 12,408), seasonal (N = 5,227) and annual (N = 1,461) means of $PM_{2.5}$ predictions are highly correlated with the surface observations with R^2 value of 0.79, 0.81, and 0.82, respectively, showing overall small estimation uncertainties (i.e., RMSE < 11.2 μg/m^3, MAE < 8.6 μg/m^3, MRE < 25.8 μg/m^3) across China. These results illustrate that the STET model has a strong predictive power and can well capture the historical $PM_{2.5}$ concentrations across China.

[Please insert Figure 9 here]

4.3 Predicted $PM_{2.5}$ maps across China

The monthly $PM_{2.5}$ maps are synthesized and averaged from at least 20% available daily $PM_{2.5}$ estimates for each grid in a month in 2018 across China (Hsu et al., 2012). The monthly $PM_{2.5}$ estimates and ground measurements (N = 12,411) are highly correlated (R^2 = 0.94) with a stronger slope of 0.94. The average RMSE and MAE are 5.35 and 3.87 μg/m^3, respectively. The monthly spatial coverage varies from 73 to 92%, with an average of 83% across China. The highest (lowest) spatial coverage occcurs around October (January) of the year. Similarly, the monthly mean $PM_{2.5}$ values vary conversely from 21.2 to 45.1 μg/m^3 with the highest (lowest) $PM_{2.5}$ concentration occurring around March (August) of the year.

Figure 10a shows the annual $PM_{2.5}$ maps across China which are generated from monthly $PM_{2.5}$ maps if there are more than eight available values for each grid in 2018 (Wei et al., 2019d). The spatial patterns are similar between the STET-derived 1-km $PM_{2.5}$ map and calculated in-situ measurements (Figure 10b). In addition, validation results suggest that the annual mean $PM_{2.5}$ estimates (N = 1,461) are highly consistent with ground measurements (R = 0.93) with small uncertainties (i.e., RMSE = 3.82 and MAE = 2.90 μg/m^3). This illustrate that the synthetic dataset can more accurately reflect the annual $PM_{2.5}$ loadings across China.

The average $PM_{2.5}$ concentration is 33.9±16.3 μg/m^3 in 2018 across mainland China. In general, the most severe $PM_{2.5}$ pollution occurs in the Taklamakan Deseret, where most areas expose high $PM_{2.5}$

concentrations > 80 μg/m^3. There are also high-polluted levels over the North China Plain, Sichuan Basin, and Yangtze River Delta, with annual mean $PM_{2.5}$ values of 46.8±11.8, 38.3±10.3, and 37.6±9.4 μg/m^3, respectively. These mainly contributed to intensive human activities, special topographic and meteorological conditions. By contrast, the annual mean $PM_{2.5}$ loadings are overall low in the rest areas of China, e.g., Pearl River Delta (30.5±5.0 μg/m^3). However, there may be poor representativeness for these areas over western China with few ground monitoring stations. In general, we have to say that the $PM_{2.5}$ pollution has been significantly reduced in 2018 across China due to the effective emission control measures implemented by the Chinese government (Fang et al., 2019; Ma et al., 2019). However, more than 30% of mainland China still experienced high $PM_{2.5}$ levels exceeding the recommended air quality level ($PM_{2.5}$ > 35 μg/m^3).

[Please insert Figure 10 here]

Figure 11 shows seasonal mean $PM_{2.5}$ maps, which are averaged from the available monthly values for each grid, in 2018 across China. Preliminary validation against surface measurements suggest that the seasonal mean $PM_{2.5}$ estimates are in good accuracy (i.e., R^2 = 0.94, RMSE = 4.72 μg/m^3, and MAE = 3.49 μg/m^3), which can better describe the seasonal variations in $PM_{2.5}$ concentrations across China. There are noticeable spatial differences in $PM_{2.5}$ distributions on the seasonal scale. In winter and spring, more than 77% and 66% of mainland China exposing the high $PM_{2.5}$ levels > 30 μg/m^3, yielding poorer air quality. By contrast, $PM_{2.5}$ pollution is slighter in summer and autumn with more than 91% and 81% of mainland China experiencing low $PM_{2.5}$ levels below the acceptable air quality level. Note that in spring, $PM_{2.5}$ concentrations are particularly high in Xinjiang province due to frequent sand and dust episodes in 2018.

[Please insert Figure 11 here]

4.4 Comparison with related studies

There is an increasing number of studies on estimating $PM_{2.5}$ using satellite AOD products from local to national scales across China. However, limited by the operational satellite aerosol products, $PM_{2.5}$ can only be estimated at coarse spatial resolutions of approximately 6–10 km (Fang et al., 2016; Li et al.,

https://doi.org/10.5194/acp-2019-815
Preprint. Discussion started: 23 October 2019

2017b; Yu et al., 2017; Chen et al., 2018; Ma et al., 2019; Yao et al., 2019). Recently, with the release of MODIS 3-km DT aerosol products, the $PM_{2.5}$ estimates can be improved to 3-km spatial resolution across China (You et al., 2016; Li et al., 2017a; He & Huang, 2018; Chen et al., 2019; Xue et al., 2019). Therefore, in our study, the spatial resolution of $PM_{2.5}$ estimates has been significantly improved by 3–10 times to 1 km based on the newly released high-quality MAIAC products across mainland China. For model performance, our newly developed STET model shows much higher accuracy with higher CV-R^2 values, smaller RMSE and MAE values than the statistical regression models (Table 2), e.g., the timely structure adaptive model (TSAM, Fang et al., 2016) model, the Gaussian model (Yu et al., 2017), the Generalized Additive Model (GAM, Chen et al., 2018) model, and the GWR model (Ma et al., 2014; You et al., 2016), and the GTWR model (He and Huang, 2018). The STET model can also outperform most machine learning (ML) and deep learning approaches including the RF model (Chen et al., 2018; Wei et al., 2019e), the XGBoost model (Chen et al., 2019), the Geo- BPNN, GRNN and deep brief network (DBN) models (Li et al., 2017a, 2017b), and some optical combined models, e.g., the Daily-GWR (D-GWR) model (He and Huang, 2018), the two-stage model (He and Huang, 2018; Ma et al., 2019; Yao et al., 2019), and the ML + GAM model (Xue et al., 2019). In addition, there are only a hanful of studies on the predictive power in $PM_{2.5}$ concentrations across China. The comparison results show that our STET model is superior to those results reported by previous studies, i.e., the two-stage model (Ma et al., 2019), the GTWR model (He and Huang, 2018), the ML + GAM model (Xue et al., 2019), and the STRF model (Wei et al., 2019e).

[Please insert Table 2 here]

5. Summary and conclusion

With the increase in air pollution over recent years, abundant studies on estimating $PM_{2.5}$ have been performed using satellite remote sensing. However, most of the $PM_{2.5}$ estimates are reported at spatial resolutions of 3–10 km, which is inadequate for monitoring air quality at urban areas. The accuracy of $PM_{2.5}$ estimates is also limited by traditional models. Therefore, we try to generate high-quality $PM_{2.5}$ maps at 1-km higher spatial resolution across China. For this, a new space-time extremely randomized

https://doi.org/10.5194/acp-2019-815
Preprint. Discussion started: 23 October 2019

trees (STET) approach is developed to minimize the spatiotemporal heterogeneities in $PM_{2.5}$ and improve the estimate accuracy.

Our results suggest that the STET model shows great performance in estimating daily $PM_{2.5}$ concentrations with a relatively high sample-based cross-validation coefficient of 0.89, low RMSE of 10.35 μg/m^3, MAE of 6.71 μg/m^3 and MRE of 21.37% at the national scale. Comparisons illustrate that spatiotemporal information is of great importance and should be carefully considered during model development. The STET model shows better performance at most monitoring stations and individual days in the year. The North China Plain and the Sichuan Basin regions, under the influence of intense human activities and poor dispersion conditions, have high $PM_{2.5}$ loadings. Moreover, the STET model can outperform most models presented in previous related studies in terms of spatial resolution, model accuracy and predictive power. This study suggests that the 1-km-resolution $PM_{2.5}$ dataset will be of great importance in future atmospheric pollution focused on medium- or small-scale areas. In addition, the STET model will be applied to produce the historical $PM_{2.5}$ dataset across China in our future studies since MODIS can cover global observations nearly over the past 20 years.

Data availability

Data are available by contacting the author (weijing_rs@163.com).

Author contributions

ZL designed the research, and JW carried out the research and wrote the initial draft of this manuscript. WX, LX, LL, HW, and YS helped collected and processed the used data. ZL, LS, JG, YP, and JL helped review the manuscript. All authors made substantial contributions to this work.

Competing interests

The authors declare that they have no conflict of interest.

Acknowledgements

The in-situ $PM_{2.5}$ measurements are available from the China National Environmental Monitoring Center (http://www.cnemc.cn). The MODIS series products are available at https://search.earthdata.nasa.gov/, and the ERA-Interim reanalysis products are available at https://www.ecmwf.int/en/forecasts/datasets/reanalysis-datasets/era-interim. The AERONET measurements are available at https://aeronet.gsfc.nasa.gov/.

Financial support

This research has been supported by the National Key R&D Program of China (2017YFC1501702), the National Natural Science Foundation of China (91544217), the U.S. National Science Foundation (AGS1534670), and the BNU Interdisciplinary Research Foundation for the First-Year Doctoral Candidates (BNUXKJC1808).

References

Aggarwal, P., & Jain, S.: Impact of air pollutants from surface transport sources on human health: a modeling and epidemiological approach. Environment International, 83, 146-157, 2015.

Bartell, S. M., Longhurst, J., Tjoa, T., Sioutas, C., and Delfino, R. J.: Particulate air pollution, ambulatory heart rate variability, and cardiac arrhythmia in retirement community residents with coronary artery disease. Environmental Health Perspectives, 121(10), 1135–1141, 2013.

Brokamp, C., Jandarov, R., Hossain, M., Ryan, P.: Predicting daily urban fine particulate matter concentrations using a random forest model. Environmental Science and Technology, 52 (7), 4173–4179, 2018.

Chen, G., Li, S., Knibbs, L., Hamm, N., Cao, W., Li, T., Guo, J., Ren, H., Abramson, M., Guo, Y.: A machine learning method to estimate $PM_{2.5}$, concentrations across China with remote sensing, meteorological and land use information. Science of The Total Environment, 636, 52-60, 2018.

Chen, Z., Zhang, T., Zhang, R., Zhu, Z., Yang, J., Chen, P., Ou, C., Guo, Y.: Extreme gradient boosting model to estimate $PM_{2.5}$ concentrations with missing-filled satellite data in China, Atmospheric Environment, 202, 180–189, 2019.

Chowdhury, S., and Dey, S.: Cause-specific premature death from ambient $PM_{2.5}$ exposure in India: estimate adjusted for baseline mortality. Environment International, 91, 283-290, 2016.

Crippa, M., Janssens-Maenhout, G., Guizzardi, D., Van Dingenen, R., and Dentener, F.: Contribution and uncertainty of sectorial and regional emissions to regional and global $PM_{2.5}$ health impacts, Atmospheric Chemistry and Physics, 19, 5165–5186, 2019.

Fang, D., Chen, B., Hubacek, K., Ni, R., Chen, L., Feng, K., Lin, J.: Clean air for some: Unintended spillover effects of regional air pollution policies. Science Advances, 5, 1-10, 2019.

Geurts, P., Ernst, D., Wehenkel, L.: Extremely randomized trees, Machine Leaning, 63(1), 3-42, 2006.

Guo, J., Zhang, X., Che, H., Gong, S., An, X., Cao, C., Guang, J., Zhang, H., Wang, Y., Zhang, X., Xue, M., Li, X.: Correlation between PM concentrations and aerosol optical depth in eastern china. Atmospheric Environment, 43(37), 5876-5886, 2009.

Guo, J., Xia, F., Zhang, Y., Liu, H., Li, J., Lou, M, He, J., Yan, Y., Wang, F., Min, M., Zhai, P.: Impact of diurnal variability and meteorological factors on the $PM_{2.5}$-AOD relationship: implications for $PM_{2.5}$ remote sensing. Environmental Pollution, 221(94), 94, 2017.

Gupta, P., and Christopher, S.: Particulate matter air quality assessment using integrated surface, satellite, and meteorological products: multiple regression approach. Journal of Geophysical Research: Atmospheres, 114(D14205). doi:10.1029/2008JD011496, 2009.

Han, L., Zhou, W., Li, W., and Li, L.: Impact of urbanization level on urban air quality: a case of fine particles ($PM_{2.5}$) in Chinese cities. Environmental Pollution, 194, 163-170, 2014.

He, K., Hong Huo, A., and Zhang, Q.: Urban air pollution in China: current status, characteristics, and progress. Annual Review of Energy & the Environment, 27(1), 397-431, 2011.

He, Q., and Huang, B.: Satellite-based mapping of daily high-resolution ground $PM_{2.5}$ in China via space-time regression modeling. Remote Sensing of Environment, 206, 72–83, 2018.

Atmospheric Chemistry and Physics Discussions
Open Access
EGU

Hsu, N., Gautam, R., Sayer, A., Bettenhausen, C., Li, C., Jeong, M. J., Tsay, S., and Holben, B.: Global and regional trends of aerosol optical depth over land and ocean using SeaWiFS measurements from 1997 to 2010. Atmospheric Chemistry and Physics, 12, 8037-8053, 2012.

Hu, X., Belle, J.H., Meng, X., Wildani, A., Waller, L., Strickland, M., Liu, Y.: Estimating $PM_{2.5}$ concentrations in the conterminous united states using the random forest approach. Environmental Science and Technology, 51(12), 6936–6944, 2017.

Huang, R., Zhang, Y., Bozzetti, C., Ho, K., Cao, J., Han, Y., Daellenbach, K., Slowik, J., Platt, S., Canonaco, F., Zotter, P., Wolf, R., Pieber, S., Bruns, E., Cripa, M., Ciarelli, G., Piazzalunga, A., Schwikowski, M., Abbaszade, G., Schnelle-Kreis, J., Zimmermann, R., An, Z., Szidat., S., Baltensperger, U., Haddad, I., Prevot, A.: High secondary aerosol contribution to particulate pollution during haze events in China. Nature, 514(7521), 218-222, 2014.

Koren, I., Dagan, G., Altaratz, O.: From aerosol-limited to invigoration of warm convective clouds. Science, 344, 1143-1146, 2014.

Levy, R. C., S. Mattoo, L. A. Munchak, L. A. Remer, A. M. Sayer, F. Patadia, & N. C. Hsu.: The Collection 6 MODIS aerosol products over land and ocean. Atmospheric Measurement Techniques, 6, 2989–3034, 2013.

Li, T., Shen, H., Zeng, C., Yuan, Q., and Zhang, L.: Point-surface fusion of station measurements and satellite observations for mapping $PM_{2.5}$ distribution in China: methods and assessment. Atmospheric Environment, 152, 477–489, 2017a.

Li, T., Shen, H., Yuan, Q., Zhang, X., and Zhang, L.: Estimating ground-level $PM_{2.5}$ by fusing satellite and station observations: A geo-intelligent deep learning approach. Geophysical Research Letters, 44(23), 11985-11993, 2017b.

Liu, M., Huang, Y., Ma, Z., Jin, Z., Liu, X., Wang, H., Liu, Y., Wang, J., Jantunen, M., Bi, J., Dr., P.: Spatial and temporal trends in the mortality burden of air pollution in China: 2004-2012. Environment International, 98, 75-81, 2017.

Liu, N., Zou, B., Feng, H., Wang, W., Tang, Y., and Liang, Y.: Evaluation and comparison of multiangle implementation of the atmospheric correction algorithm, Dark Target, and Deep Blue aerosol products over China, Atmospheric Chemistry and Physics, 19, 8243-8268, 2019.

https://doi.org/10.5194/acp-2019-815
Preprint. Discussion started: 23 October 2019

Li, Z., Guo, J., Ding, A., Liao, H., Liu, J., Sun, Y., Wang, T., Xue, H., Zhang, H., Zhu, B.: Aerosol and boundary-layer interactions and impact on air quality. National Science Review, 4(6), 810-833, 2017.

Lyapustin, A., Wang, Y., Laszlo, I., Kahn, R., Korkin, S., Remer, L., Levy, R., Reid, J.: Multiangle implementation of atmospheric correction (MAIAC): 2. aerosol algorithm. Journal of Geophysical Research: Atmospheres, 116. https://doi.org/10.1029/2010JD014985, 2011.

Lyapustin, A., Wang, Y., Korkin, S., and Huang, D.: MODIS Collection 6 MAIAC algorithm, Atmospheric Measurement Techniques, 11, 5741–5765, 2018.

Ma, Z., Hu, X., Huang, L., Bi, J., and Liu, Y.: Estimating ground-level $PM_{2.5}$ in China using satellite remote sensing. Environmental Science and Technology, 48(13), 7436–7444, 2014.

Ma, Z., Liu, R., Liu, Y., and Bi, J.: Effects of air pollution control policies on $PM_{2.5}$ pollution improvement in China from 2005 to 2017: a satellite-based perspective. Atmospheric Chemistry and Physics, 19, 6861–6877, 2019.

Peng, R. D., Bell, M. L., Geyh, A. S., McDermott, A., Zeger, S. L., Samet, J. M., and Dominici, F.: Emergency admissions for cardiovascular and respiratory diseases and the chemical composition of fine particle air pollution. Environmental Health Perspectives, 117(6), 957–963, 2009.

Rodriguez, J. D., Perez, A., and Lozano, J. A.: Sensitivity analysis of k-fold cross validation in prediction error estimation. IEEE Transactions on Pattern Analysis and Machine Intelligence, 32(3), 569–575, 2010.

Seinfeld, J. H., Bretherton, C., Carslaw, K. S., Coe, H., Demott, P. J., Dunlea, E. J., Feingold, G., Ghan, S., Chan, S., Guenther, A., Kahn, R., Kredenweis, S., Molina, M., Nenes, A., Penner, J., Prather, K., Ramanathan, V., Ramaswamy, V., Rashch, P., Ravishankara, A.: Improving our fundamental understanding of the role of aerosol-cloud interactions in the climate system. Proceedings of the National Academy of Sciences, 113(21), 5781-5790, 2016.

Silva, R., West, J., Zhang, Y., Anenberg, S., Lamarque, J., Shindell, D., Collins, W., Dalsøren, S., Faluvegi, G., Folberth, G., Horowitz, L., Nagashima, T., Naik, V., Rumbold, S., Skeie, R., Sudo, K., Takemura, T., Bergmann, D., Cameron-Smith, P., Cionni, I., Doherty, R., Eyring, V., Josse, B., MacKenzie, I., Plummer, D., Righi, M., Stevenson, D., Strode, S., Szopa, S., Zeng, G.: Global

https://doi.org/10.5194/acp-2019-815
Preprint. Discussion started: 23 October 2019

Atmospheric Chemistry and Physics Discussions

premature mortality due to anthropogenic outdoor air pollution and the contribution of past climate change. Environmental Research Letters, 8(3), 034005, 2013.

Song, Y., Huang, B., He, Q., Chen, B., Wei, J., and Mahmood, R.: Dynamic assessment of $PM_{2.5}$ exposure and health risk using remote sensing and geo-spatial big data. Environmental Pollution, 253: 288-296, 2019.

Sun, L., Wei, J., Duan, D., Guo, Y., Yang, D., Jia, C. and Mi, X.: Impact of land-use and land-cover change on urban air quality in representative cities of China. Journal of Atmospheric and Solar-Terrestrial Physics, 142, 43–54, 2016.

Tao, M., Wang, J., Li, R., Wang, L., Wang, L., Wang, Z., Tao, J., Che, H., Chen, L.: Performance of MODIS high-resolution MAIAC aerosol algorithm in China: Characterization and limitation, Atmospheric Environment, 213, 159–169, 2019.

Wei, J., Sun, L., Huang, B., Bilal, M., Zhang, Z., and Wang, L.: Verification, improvement and application of aerosol optical depths in China. Part 1: Inter-comparison of NPP-VIIRS and Aqua-MODIS, Atmospheric Environment, 175, 221–233, 2018.

Wei, J., Li, Z., Sun, L., Peng, Y., Wang, L.: Improved merge schemes for MODIS Collection 6.1 Dark Target and Deep Blue combined aerosol products. Atmospheric Environment, 202, 315–327, 2019a.

Wei, J., Li, Z., Peng, Y., and Sun, L.: MODIS Collection 6.1 aerosol optical depth products over land and ocean: validation and comparison, Atmospheric Environment, 201, 428–440, 2019b.

Wei, J., Li, Z., Peng, Y., Sun, L., and Yan, X.: A regionally robust high-spatial-resolution aerosol retrieval algorithm for MODIS images over Eastern China, IEEE Transactions and Geoscience Remote Sensing, 57(7), 4748-4757, 2019c.

Wei, J., Peng, Y., Mahmood, R., Sun, L., and Guo, J.: Intercomparison in spatial distributions and temporal trends derived from multi-source satellite aerosol products, Atmospheric Chemistry and Physics, 19, 7183-7207, 2019d.

Wei, J., Huang, W., Li, Z., Xue, W., Peng, Y., Sun, L., and Cribb, M.: Estimating 1-km-resolution $PM_{2.5}$ concentrations across China using the space-time random forest approach, Remote Sensing of Environment, 231, 1-14, 2019e.

https://doi.org/10.5194/acp-2019-815
Preprint. Discussion started: 23 October 2019

Wu, J., Zheng, H., Zhe, F., Xie, W., and Song, J.: Study on the relationship between urbanization and fine particulate matter ($PM_{2.5}$) concentration and its implication in China. Journal of Cleaner Production, 182, 872-882, 2018.

Xiao, Q., Wang, Y., Chang, H. H., Meng, X., Geng, G., Lyapustin, A., and Liu, Y.: Full-coverage high-resolution daily $PM_{2.5}$ estimation using MAIAC AOD in the Yangtze River Delta of China. Remote Sensing of Environment, 199, 437–446, 2017.

Xue, T., Zheng, Y., Tong, D., Zheng, B., Li, X., Zhu, T., and Zhang, Q.: Spatiotemporal continuous estimates of $PM_{2.5}$ concentrations in China, 2000–2016: A machine learning method with inputs from satellites, chemical transport model, and ground observations. Environment International, 123, 345-357, 2019.

Yao, F., Wu, J., Li, W., and Peng, J.: A spatially structured adaptive two-stage model for retrieving ground-level $PM_{2.5}$ concentrations from VIIRS AOD in China. ISPRS Journal of Photogrammetry and Remote Sensing, 151, 263-276, 2019.

You, W., Zang, Z., Zhang, L., Li, Y., Pan, X., and Wang, W.: National-scale estimates of ground-level $PM_{2.5}$ concentration in China using geographically weighted regression based on 3-km resolution MODIS AOD. Remote Sensing, 8(3), 184, 2016.

Zhai, S., Jacob, D., Wang, X., Shen, L., Li, K., Zhang, Y., Gui, K., Zhang, T., and Liao, H.: Fine particulate matter ($PM_{2.5}$) trends in China, 2013–2018: separating contributions from anthropogenic emissions and meteorology. Atmospheric Chemistry and Physics, 19, 11031-11041, 2019.

Zhang, Y., and Li, Z.: Remote sensing of atmospheric fine particulate matter ($PM_{2.5}$) mass concentration near the ground from satellite observation. Remote Sensing of Environment, 160, 252-262, 2015.

Zhang, Z., Wu, W., Fan, M., Wei, J., Tan, Y., and Wang, Q.: Evaluation of MAIAC aerosol retrievals over China. Atmospheric Environment, 202, 8-16, 2019.

https://doi.org/10.5194/acp-2019-815
Preprint. Discussion started: 23 October 2019

Atmospheric Chemistry and Physics Discussions

595 Table 1. Summary of the data sources used in this study.

Dataset	Variable	Content	Unit	Spatial Resolution	Temporal Resolution	Data source
PM_1	$PM_{2.5}$	$PM_{2.5}$	μg/m^3	-	Hourly	CNEMC
AOD	AOD	MAIAC AOD	-	1 km ×1 km	Daily	MCD19A2
Meteorological data	BLH	Boundary layer height	m	0.125°×0.125°	3-hour	ERA-Interim reanalysis product
	PRE	Total precipitation	mm	0.125°×0.125°	3-hour	
	EP	Evaporation	mm	0.125°×0.125°	3-hour	
	RH	Relative humidity	%	0.125°×0.125°	3-hour	
	TEM	2-m air temperature	K	0.125°×0.125°	6-hour	
	SP	Surface pressure	hPa	0.125°×0.125°	6-hour	
	WS	10-m wind speed	m/s	0.125°×0.125°	6-hour	
	WD	10-m wind direction	m/s	0.125°×0.125°	6-hour	
Land cover	NDVI	NDVI	-	500 m × 500 m	Monthly	MOD13A3
	LUC	Land use cover	-	500 m × 500 m	Annually	MCD12Q1
Topography	DEM	DEM	m	90 m × 90 m	-	SRTM
	Relief	Surface relief	m	90 m × 90 m	-	
	Aspect	Surface aspect	degree	90 m × 90 m	-	
	Slope	Surface slope	degree	90 m × 90 m	-	
Population	NTL	Night lights	W/cm^2/sr	500 m × 500 m	Monthly	VIIRS

https://doi.org/10.5194/acp-2019-815
Preprint. Discussion started: 23 October 2019

Atmospheric Chemistry and Physics Discussions

Table 2. Comparison between model performances of the STET model and other models from previous related studies focused on China.

Model	Resolution	Model Validation			Predictive power		Literature
		R^2	RMSE	MAE	Daily	Monthly	
GWR	10 km	0.64	32.98	21.25	-	-	Ma et al., (2014)
TSAM	10 km	0.80	22.75	15.99	-	-	Fang et al. (2016)
Gaussian	10 km	0.81	21.87	-	-	-	Yu et al. (2017)
RF	10 km	0.83	18.08	-	-	-	Chen et al. (2018)
GAM		0.55	29.13	-	-	-	
Geo-BPNN	10 km	0.84	15.23	10.34	-	-	Li et al. (2017b)
Geo-GRNN		0.82	16.93	12.34	-	-	
Geo-DBN		0.88	13.03	08.54	-	-	
Two-stage	10 km	0.77	17.10	11.51	0.41	0.73	Ma et al. (2019)
Two-stage	6 km	0.60	21.76	14.41	-	-	Yao et al. (2019)
GRNN	3 km	0.67	20.93	13.90	-	-	Li et al. (2017a)
GWR	3 km	0.81	21.87	-	-	-	You et al. (2017)
D-GWR	3 km	0.72	21.01	14.59	-	-	He & Huang (2018)
Two-stage		0.71	21.21	13.50	-	-	
GTWR		0.80	18.00	12.03	0.41	-	
XGBoost	3 km	0.86	14.98	-	-	-	Chen et al. (2019)
ML + GAM	3 km	0.61	27.80	17.70	0.57	0.74	Xue et al. (2019)
STRF	1 km	0.85	15.57	9.77	0.55	0.73	Wei et al. (2019e)
STET	1 km	0.89	10.35	6.71	0.60	0.80	Our study

Atmospheric Chemistry and Physics Discussions

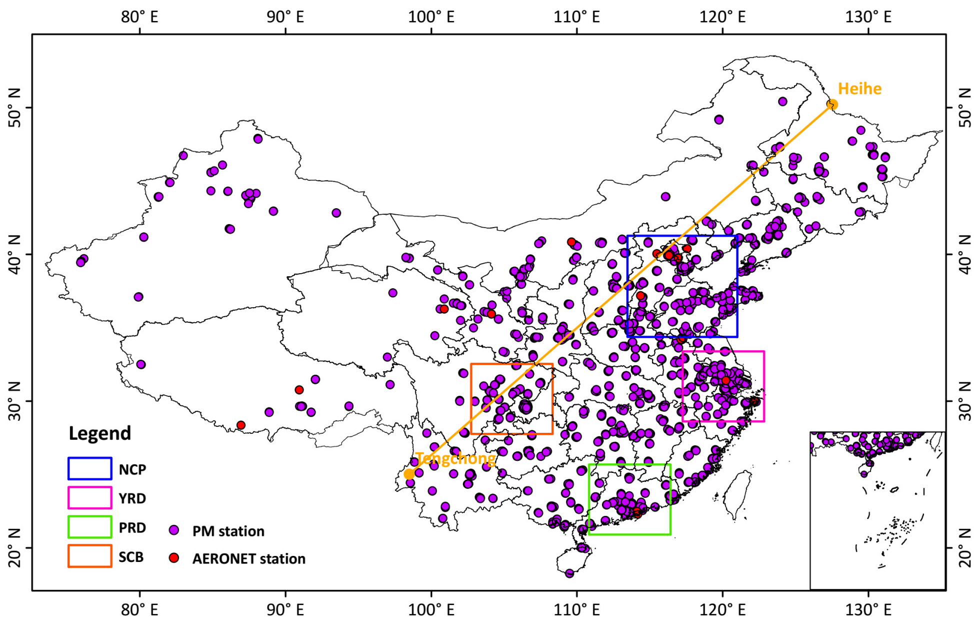

Figure 1. Spatial distributions of $PM_{2.5}$ and AERONET monitoring stations in China. The Heihe-Tengchong line (orange line) shows the boundary between Eastern and Western China.

https://doi.org/10.5194/acp-2019-815
Preprint. Discussion started: 23 October 2019

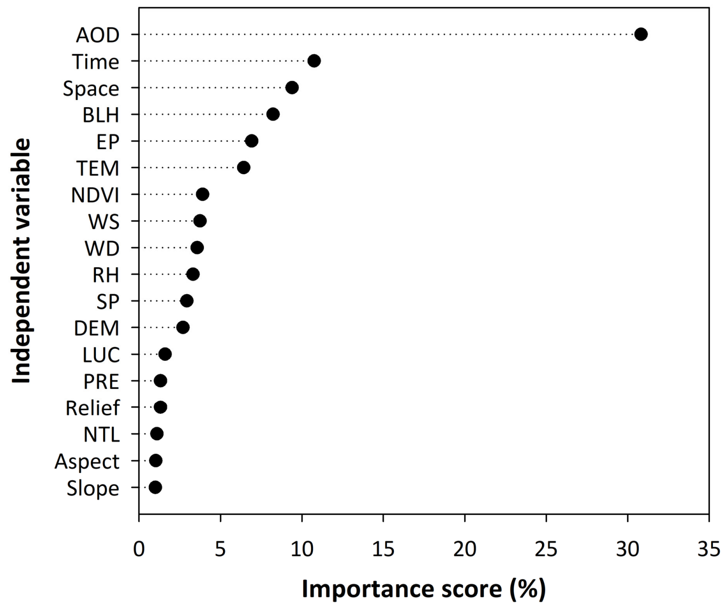

605 Figure 2. Importance score (%) of independent variables to $PM_{2.5}$ estimates for the STET model.

https://doi.org/10.5194/acp-2019-815
Preprint. Discussion started: 23 October 2019

Atmospheric Chemistry and Physics Discussions

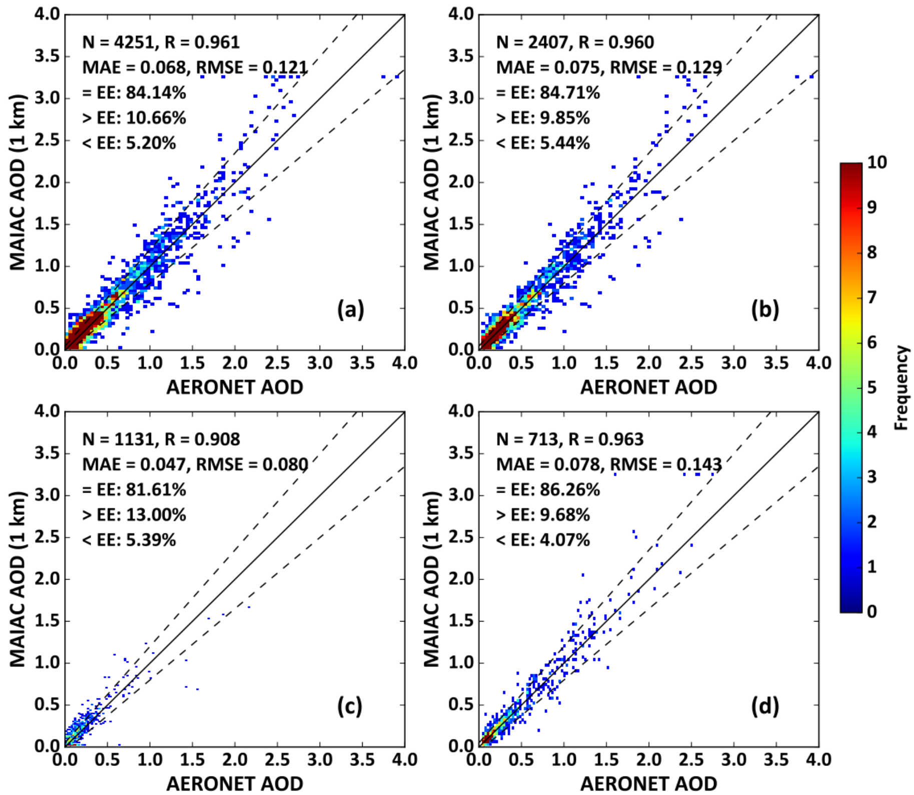

610 Figure 3. Scatter plots of MAIAC AOD retrievals versus AERONET AODs at 550 nm in (a) China, and (b) urban, (c) cropland, and (d) grassland. The dotted lines represent the upper and lower boundaries of the expected error (EE).

https://doi.org/10.5194/acp-2019-815
Preprint. Discussion started: 23 October 2019

Atmospheric Chemistry and Physics Discussions

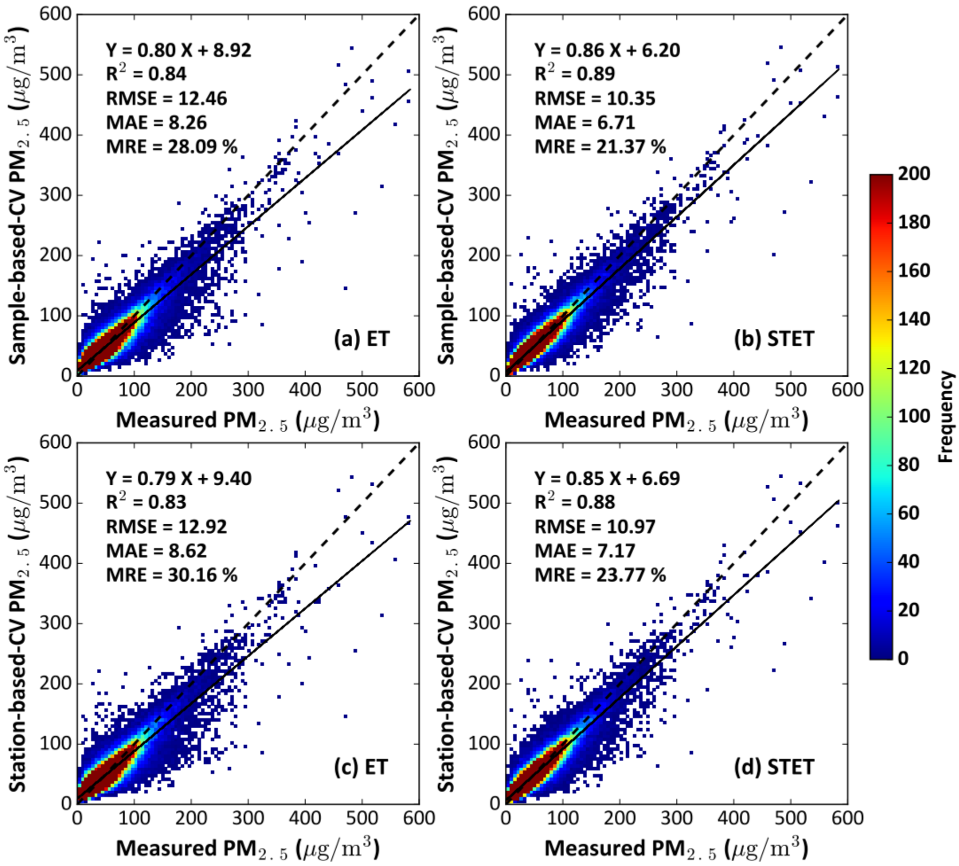

Figure 4. Density scatter plots of sample-based (top row) and station-based (bottom row) 10-CV results for the ET and STET models at the daily level (N = 167,692) in 2018 across mainland China.

https://doi.org/10.5194/acp-2019-815
Preprint. Discussion started: 23 October 2019

Atmospheric Chemistry and Physics
Discussions

615

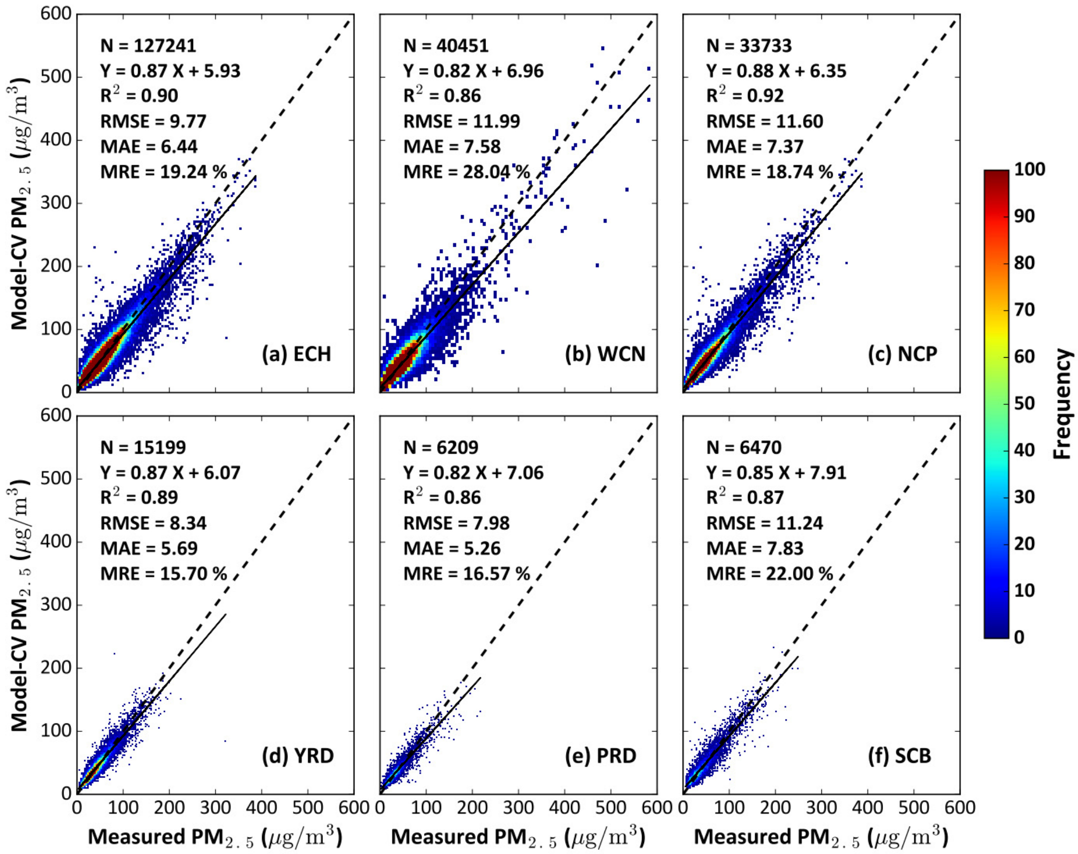

Figure 5. Density scatter plots of sample-based 10-CV results for (a) eastern China (ECH), (b) western China (WCH), (c) North China Plain (NCP), (d) Yangtze River Delta (YRD), (e) Pearl River Delta (PRD), and (f) Sichuan Basin (SCB) in 2018.

https://doi.org/10.5194/acp-2019-815
Preprint. Discussion started: 23 October 2019

Atmospheric Chemistry and Physics
Discussions

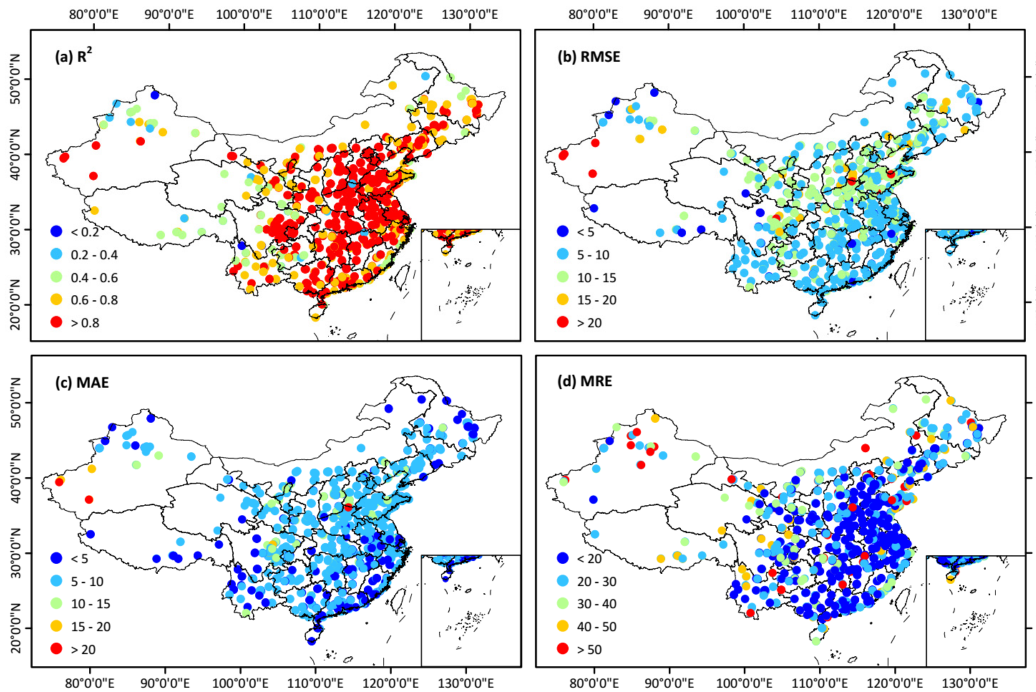

620 Figure 6. Spatial distributions of the site-scale performance of the STET model for (a) the sample-based CV-R^2, (b) RMSE, (c) MAE, and (d) MRE in 2018 across China.

https://doi.org/10.5194/acp-2019-815
Preprint. Discussion started: 23 October 2019

Atmospheric Chemistry and Physics Discussions

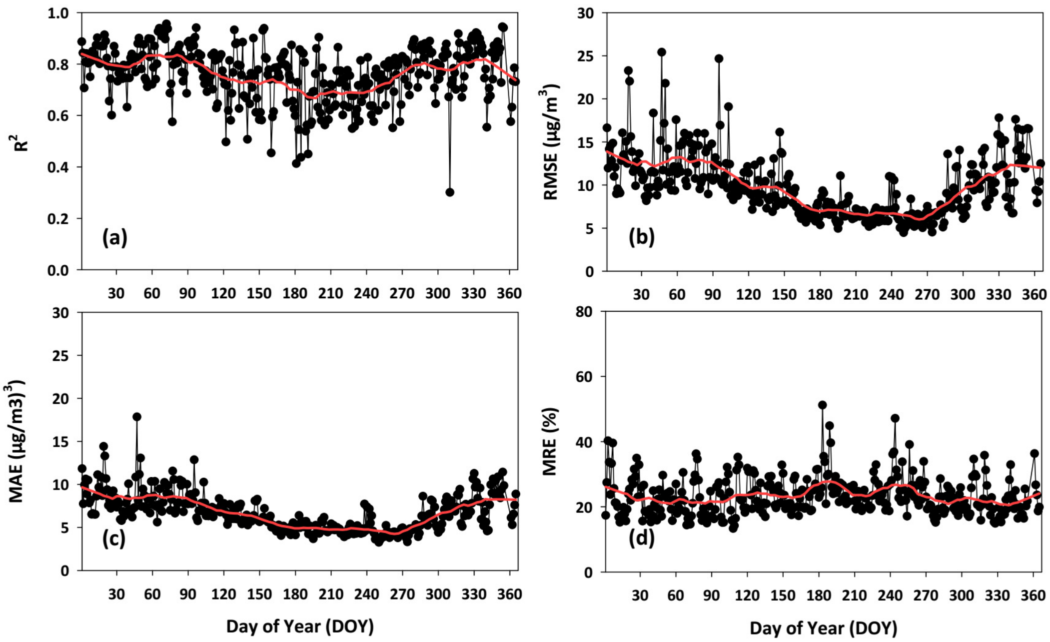

Figure 7. Time series of the daily performance of the STET model in terms of (a) sample-based CV-R^2, (b) RMSE, (c) MAE, and (d) MRE in 2018 across China

https://doi.org/10.5194/acp-2019-815
Preprint. Discussion started: 23 October 2019

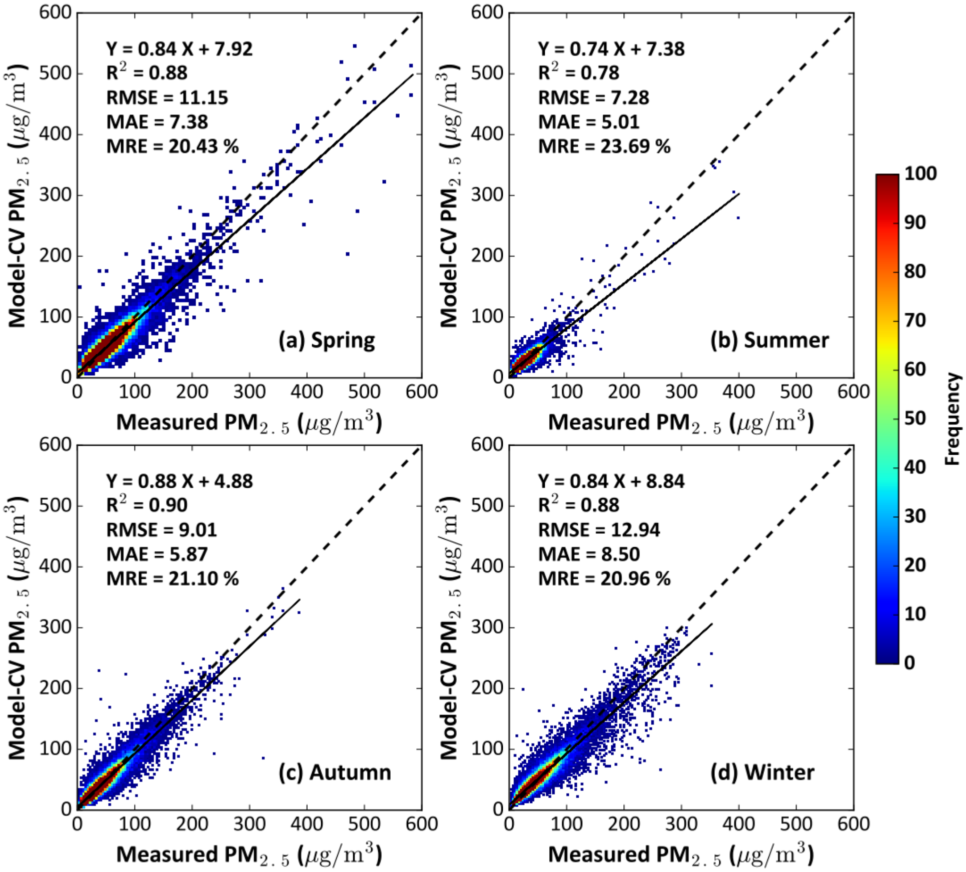

625 Figure 8. Density scatter plots of sample-based 10-CV results for the STET model for four seasons in 2018 across China.

https://doi.org/10.5194/acp-2019-815
Preprint. Discussion started: 23 October 2019

Atmospheric Chemistry and Physics
Discussions

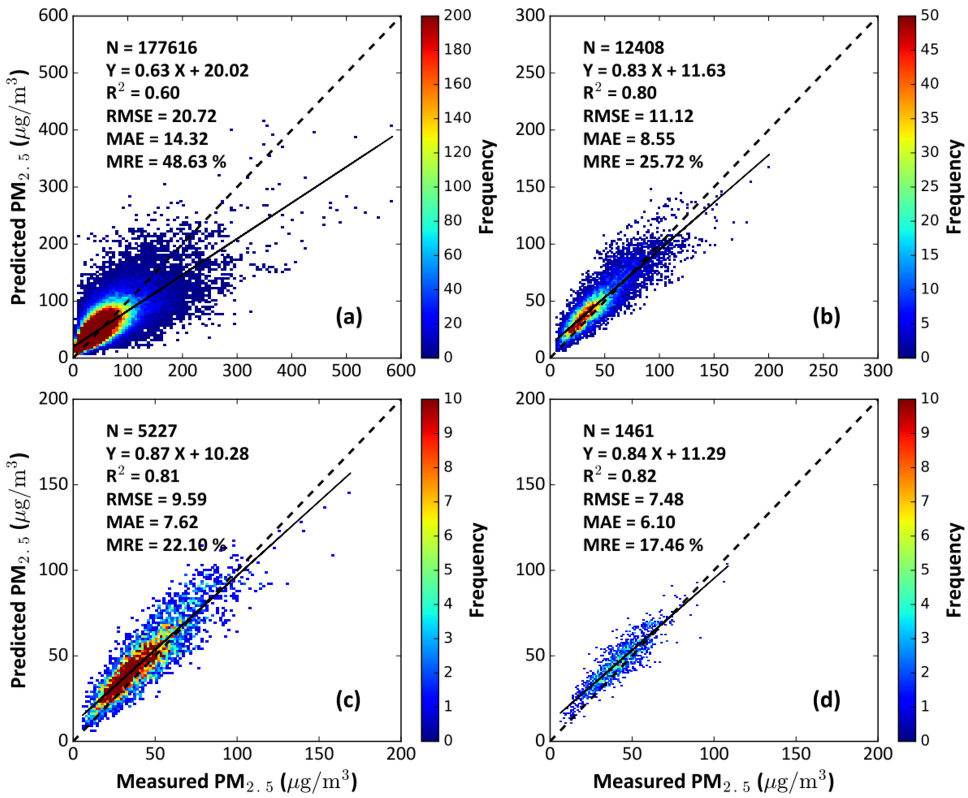

Figure 9. Density scatter plots of sample-based 10-CV results for the STET model for four seasons in 2018 across China.

https://doi.org/10.5194/acp-2019-815
Preprint. Discussion started: 23 October 2019

Atmospheric Chemistry and Physics
Discussions

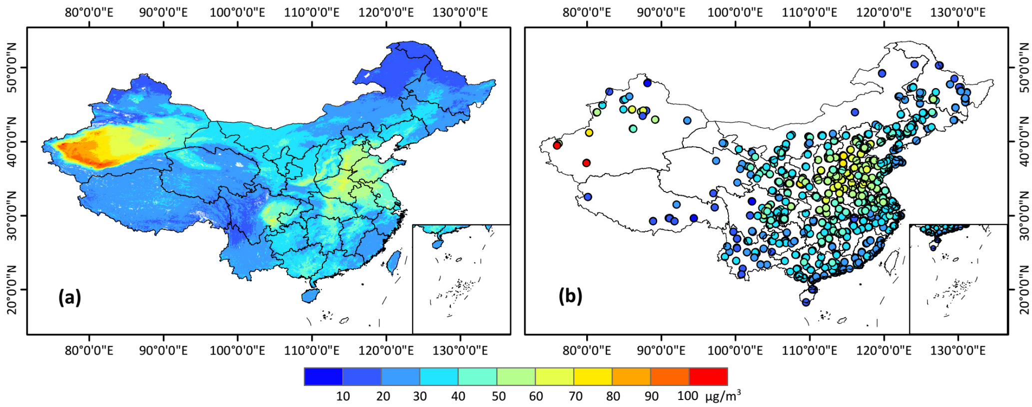

Figure 10. Spatial distributions of annual mean (a) $PM_{2.5}$ estimates and (b) surface observations in 2018 across China.

https://doi.org/10.5194/acp-2019-815
Preprint. Discussion started: 23 October 2019

Atmospheric Chemistry and Physics
Discussions

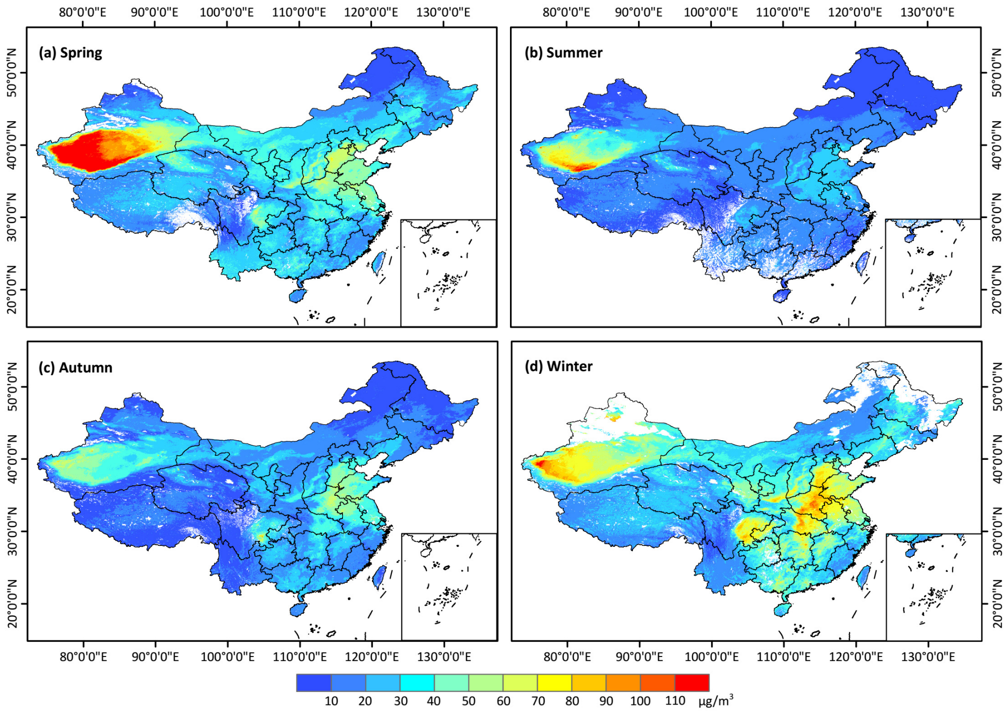

635 Figure 11. Spatial distributions of seasonal mean 1-km-resolution $PM_{2.5}$ concentrations for four seasons in 2018 across China.